

# 21cm fluctuations from primordial magnetic fields

Maresuke Shiraishi,<sup>1,2,\*</sup> Hiroyuki Tashiro,<sup>3,†</sup> and Kiyotomo Ichiki<sup>4,5,‡</sup>

<sup>1</sup>*Dipartimento di Fisica e Astronomia “G. Galilei”,*

*Università degli Studi di Padova, via Marzolo 8, I-35131, Padova, Italy*

<sup>2</sup>*INFN, Sezione di Padova, via Marzolo 8, I-35131, Padova, Italy*

<sup>3</sup>*Physics Department, Arizona State University, Tempe, Arizona 85287, USA*

<sup>4</sup>*Kobayashi-Maskawa Institute for the Origin of Particles and the Universe,  
Nagoya University, Chikusa-ku, Nagoya, 464-8602, Japan*

<sup>5</sup>*Department of Physics and Astrophysics, Nagoya University, Nagoya 464-8602, Japan*

(Dated: September 21, 2021)

Recent observations of magnetic fields in intergalactic void regions and in high redshift galaxies may indicate that large scale magnetic fields have a primordial origin. If primordial magnetic fields were present soon after the recombination epoch, they would have induced density fluctuations on the one hand and dissipated their energy into the primordial gas on the other, and thereby significantly alter the thermal history of the Universe. Here we consider both the effects and calculate the brightness temperature fluctuations of the 21cm line using simple Monte Carlo simulations. We find that the fluctuations of the 21cm line from the energy dissipation appear only on very small scales and those from the density fluctuations always dominate on observationally relevant angular scales.

## I. INTRODUCTION

Numerous astronomical observations have suggested that magnetic fields are ubiquitous in the Universe. They exist not only in galaxies, but also in even larger systems, such as in clusters of galaxies. The origin of such large scale magnetic fields is still a matter of debate [1–3]. It is now believed that the magnetohydrodynamics (MHD) dynamo is a very powerful mechanism to amplify and maintain the galactic magnetic fields. However, the dynamo mechanism does not explain the origin of magnetic fields itself. It is shown that the seed fields as large as  $10^{-20} \sim 10^{-30}$  G are necessary to explain the observed magnetic fields of  $10^{-6}$  G in galaxies and clusters of galaxies [4].

Primordial magnetic fields have been intensively studied in the literature as a possible origin of the large scale magnetic fields. A variety of mechanisms to generate the primordial magnetic fields have been proposed, which include inflation with a break of conformal invariance [5–11], effects at phase transitions in the early Universe [12–18], and cosmological vector modes in first and/or second order cosmological perturbations [19–30]. The field strength of generated magnetic fields varies depending on the proposed models, and the fields are often parametrized by the magnetic field amplitude normalized at  $\lambda = 1$  Mpc scale  $B_\lambda$  and the index  $n_B$  of the power spectrum of magnetic fields.

Recent observations of magnetic fields in galaxies at high redshift [31–33] and in void regions (under discussion [34–38]) may support the hypothesis that the seed fields are of primordial origin. If this is the case, the primordial magnetic fields have influenced many kinds of cosmological processes, such as the big bang nucleosynthesis, cosmic microwave background (CMB) anisotropies, and the formation of large scale structure of the Universe (see [39] and references therein). Recently, the Planck Collaboration placed limits on primordial magnetic fields as  $B_\lambda < 3.4$  nG and  $n_B < 0$  from the temperature anisotropies at large and small angular scales [40].

In this paper, we consider the effect of primordial magnetic fields on cosmological 21cm signals during the dark age. In particular, we investigate the thermal history of the primordial hydrogen gas in the Universe by taking into account the heat injection due to the ambipolar diffusion of the magnetic fields [41]. The heat injection from the magnetic fields into the weakly ionized primordial gas will leave a unique signature in the future 21cm observations. If the heating raises the gas temperature and, hence, the spin temperature becomes high above the background CMB temperature, the 21cm signal comes as an emission even at redshift  $z \gtrsim 20$ , while the signal during the dark age is expected to be absorption in the standard thermal history of the Universe.

The global effects of the heating from primordial magnetic fields have already been studied in Refs. [41–46]. In particular, Refs. [43, 45] have investigated these global effect on the 21cm signals. They found that the evolution of

---

\*Electronic address: maresuke.shiraishi@pd.infn.it

†Electronic address: hiroyuki.tashiro@asu.edu

‡Electronic address: ichiki@phys.nagoya-u.ac.jp

gas temperature can change significantly, and the temperature rises as high as  $T_g \gtrsim 10^3$  K in redshift  $10 \lesssim z \lesssim 1000$  if nanogauss magnetic fields (comoving) are considered. Here we extend their investigations by taking the spatial fluctuations of the heat injection into account. Since it is considered that primordial magnetic fields are possibly distributed following Gaussian random statistics, we also expect that the heating rate also has fluctuations in space and nontrivial correlations. One complicated thing here is that the correlation will be highly nonlinear: one has to evaluate eight-point correlation functions of the primordial magnetic fields because the ambipolar heating term is proportional to the magnetic field values to the fourth power. In this paper we utilize simple Monte Carlo simulations to evaluate the correlation, and examine the power spectrum of the heating rate and the corresponding 21cm signal from the high redshift Universe. This is partly motivated by the fact that proposed future observations of HI gas in high redshifts are performed by interferometers such as the Square Kilometer Array (SKA), and therefore signals with contrast, i.e., fluctuations, are easier to detect than the global ones. Throughout this paper, we adopt the standard  $\Lambda$ CDM model with  $h = 0.7$ ,  $\Omega_b h^2 = 0.0223$ , and  $\Omega_c h^2 = 0.104$ , where  $h$  is the present Hubble constant normalized by 100 km/s/Mpc and  $\Omega_b$  and  $\Omega_c$  are the present baryon and cold dark matter (CDM) energy density parameters, respectively.

## II. THEORY OF AMBIPOLAR DIFFUSION IN THE DARK AGE

After the recombination epoch, magnetic fields create the difference in motion between neutral and ionized baryons by their Lorentz force. This velocity difference induces finite viscosity in the baryon fluid. As a result, the magnetic field energy is transferred to the thermal energy of baryons. This process is the so-called ambipolar diffusion [47] and can happen at the late-time Universe in the dark age under the presence of electrically neutral particles [41].

The dissipation of the magnetic field energy heats the intergalactic medium (IGM) gas, and the resultant thermal ionization becomes effective. As a result, cosmological 21cm signals are altered. In this section, we briefly review the theoretical aspects of the evolution of the IGM gas and 21cm signals with ambipolar diffusion. For simplicity, we neglect the existence of helium in the IGM gas throughout this paper.

### A. Temperature and ionization evolution of IGM gas

The energy dissipation rate due to ambipolar diffusion is given by [48]

$$\Gamma = \frac{|(\nabla \times \mathbf{B}) \times \mathbf{B}|^2}{16\pi^2 \chi \rho_b^2 x_i}, \quad (1)$$

where  $\rho_b$  is the baryon energy density and  $\chi = 3.5 \times 10^{13} \text{ cm}^3 \text{ g}^{-1} \text{ s}^{-1}$  denotes the drag coefficient [49].

The evolutions of the hydrogen gas temperature  $T_g$  are given by [41]

$$\frac{dT_g}{dt} = -2HT_g + \frac{x_i}{1+x_i} \frac{8\rho_\gamma \sigma_T}{3m_e c} (T_\gamma - T_g) + \frac{\Gamma}{1.5k_B n_H}, \quad (2)$$

where  $k_B$ ,  $\rho_\gamma$ ,  $H$ ,  $x_i$ ,  $n_H$ ,  $m_e$  and  $\sigma_T$  denote the Boltzmann constant, the photon energy density, the Hubble parameter, the ionization fraction, the hydrogen number density, the electron mass, and the cross section of Thomson scattering, respectively. The dissipation of primordial magnetic fields after the recombination epoch is also induced by the nonlinear decaying of MHD modes. This dissipation is effective around  $z > 800$  [41, 46]. Since we are interested in redshifts  $z \sim 20$  which are the observable redshifts for future 21cm observations, we neglect the dissipation due to the MHD decaying.

The evolution of the hydrogen ionization fraction is determined by photoionization by the CMB, radiative recombination and thermal collisional ionization,

$$\frac{dx_i}{dt} = \left[ \beta_e (1 - x_i) \exp\left(-\frac{h\nu_\alpha}{k_B T_\gamma}\right) - \alpha_e n_H x_i^2 \right] C + \gamma_e n_H (1 - x_i) x_i, \quad (3)$$

where  $\alpha_e$  is the recombination coefficient,  $\beta_e$  is the photo ionization coefficient,  $\gamma_e$  is the collisional ionization coefficient, and  $h\nu_\alpha = 13.6 \text{ eV}$  is the ground state binding energy of hydrogen. For these coefficients and  $C$ , we refer to Refs. [50, 51].

Although primordial magnetic fields are not detected yet, it is generally expected that the fields are tangled. Therefore, the dissipation rate  $\Gamma$  could be spatially fluctuated. The resultant temperature and ionization fraction also are fluctuated following Eqs. (2) and (3).

## B. 21cm signals from IGM gas

In the Rayleigh-Jeans limit, the intensity of cosmological 21cm signals at a frequency  $\nu$  can be written in terms of the brightness temperature  $T_{21}$ ,

$$I(\nu) = \frac{2\nu^2}{c^2} k_B T_{21}(\nu). \quad (4)$$

Since the 21cm signal is observed as an emission or absorption signal against the CMB, it is useful to define the differential brightness temperature against the CMB temperature,  $\delta T_{21} = T_{21} - T_\gamma$ . The positive  $\delta T_{21}$  represents that the 21cm signal is an emission against the CMB, while the negative one means that the signal is an absorption. For a given frequency, the differential brightness temperature is given by

$$\delta T_{21} = \frac{T_s(z) - T_\gamma(z)}{1+z} (1 - e^{-\tau(z)}), \quad (5)$$

where  $z$  is the redshift corresponding to the frequency of observation,  $1+z = \nu_{21}/\nu$  with  $\nu_{21}$  denoting the frequency of the 21cm line,  $T_s(z)$  is the spin temperature, and  $\tau(z)$  is the optical depth of the IGM at  $z$ .

The optical depth of the IGM to the hyperfine transition is expressed by [52]

$$\tau(z) = \frac{3c^3 \hbar A_{10} n_{\text{HI}}}{16 k_B \nu_{21}^2 T_s H(z)}, \quad (6)$$

where  $A_{10}$  is the spontaneous emission coefficient for the transition,  $A_{10} = 2.85 \times 10^{-15} \text{ s}^{-1}$ , and  $n_{\text{HI}}$  is the number density of HI gas. The spin temperature represents the ratio of the hyperfine level populations. Since the spin temperature of the IGM is determined by the balance among absorption of CMB photons, thermal collisional excitation, and Lyman- $\alpha$  pumping [53, 54], we can obtain the spin temperature from

$$T_s = \frac{T_\gamma + y_k T_g + y_\alpha T_\alpha}{1 + y_k + y_\alpha}, \quad (7)$$

where  $T_\alpha$  is the color temperature of Ly- $\alpha$  flux, and  $y_k$  and  $y_\alpha$  are the kinetic and the Ly- $\alpha$  coupling terms, respectively [52]. Because we assume that there are no Ly- $\alpha$  sources such as stars and galaxies in our interesting redshifts for simplicity, we neglect the Ly- $\alpha$  coupling term.

As shown in the previous section, the gas temperature induced by the ambipolar diffusion depends on the fourth power of Gaussian magnetic fields. Hence, to obtain the power spectrum of the brightness temperature fluctuations, we have to evaluate an eight-point correlation function of Gaussian magnetic fields. Since computing it analytically is quite complicated, we here shall estimate by use of random realizations of magnetic fields obtained through brute-force Monte Carlo simulations.

## III. MONTE CARLO SIMULATIONS

Let us start from a situation that seed magnetic fields are created in the very early Universe, and adiabatically decay as  $\mathbf{B}(\mathbf{x}, t) = \mathbf{B}_0(\mathbf{x})/a^2$  with  $a(t)$  being the scale factor. We assume that magnetic fields are stochastically homogeneous and isotropic. Conventionally, their power spectrum at the present time is parametrized by a strength smoothed on  $\lambda = 1 \text{ Mpc}$ ,  $B_\lambda$ , and a simple power-law function with a spectral index,  $n_B$ , as [55]

$$\begin{aligned} \langle B_{0i}(\mathbf{k}) B_{0j}^*(\mathbf{p}) \rangle &= (2\pi)^3 \frac{P_B(k)}{2} \left( \delta_{ij} - \hat{k}_i \hat{k}_j \right) \delta^{(3)}(\mathbf{k} - \mathbf{p}), \\ P_B(k) &= \frac{(2\pi)^{n_B+5} B_\lambda^2}{\Gamma(\frac{n_B+3}{2}) k_\lambda^{n_B+3}} k^{n_B} \quad \text{for } k < k_c, \end{aligned} \quad (8)$$

where  $k_\lambda = 2\pi/\lambda$  and  $k_c$  is the cutoff wave number of magnetic fields.<sup>1</sup> The cutoff scale is determined by the radiation viscosity at the recombination epoch [57, 58] and given by

$$k_c = \left[ 143 \left( \frac{B_\lambda}{1 \text{ nG}} \right)^{-1} \left( \frac{h}{0.7} \right)^{1/2} \left( \frac{\Omega_b h^2}{0.021} \right)^{1/2} \right]^{2/(n_B+5)} \text{ Mpc}^{-1}, \quad (9)$$

---

<sup>1</sup> The small amplitude of  $B_\lambda$  does not mean that the induced effects are small. The total energy density associated with magnetic fields might be large enough; e.g., see Ref. [56].

in the matter dominated universe.

Practically, instead of magnetic fields, we simulate vector potentials  $\mathbf{A}(\mathbf{k})$  in  $k$  space with  $512^3$  grids, whose power spectrum reads

$$\langle A_i(\mathbf{k})A_j^*(\mathbf{p}) \rangle = (2\pi)^3 \frac{P_B(k)}{2k^2} \delta_{ij} \delta^{(3)}(\mathbf{k} - \mathbf{p}) . \quad (10)$$

Then, every off-diagonal component vanishes and, hence, numerical operations are reduced drastically in comparison with the direct simulation of magnetic fields. After that, we convert realizations of the vector potentials into those of magnetic fields following the definition of vector potentials in  $k$  space as

$$\mathbf{B}(\mathbf{k}) = i\mathbf{k} \times \mathbf{A}(\mathbf{k}) . \quad (11)$$

With  $\mathbf{B}(\mathbf{k})$  at hand, the calculation for the energy dissipation rate due to ambipolar diffusion is straightforward: we take a rotation once again in  $k$  space,  $i\mathbf{k} \times \mathbf{B}(\mathbf{k})$ , move to real space, to get  $\nabla \times \mathbf{B}(\mathbf{x})$ , take a vector product with  $\mathbf{B}(\mathbf{x})$  in real space and obtain the energy dissipation rate  $\Gamma(\mathbf{x})$  in Eq. (1). We then calculate the thermal history at every pixel for a realization of  $\Gamma(\mathbf{x})$  and estimate the power spectrum of temperature fluctuations.

Figure 1 shows an example of realizations of (the  $x$  component of) primordial magnetic fields  $B_x$  together with the corresponding gas temperature  $T_g$ , the spin temperature  $T_s$ , the 21cm brightness temperature  $T_{21}$  and the ionization fraction  $x_i$ . As is evident from the figure, distributions of these temperature fluctuations are far from the Gaussian distributions even though magnetic fields are Gaussian distributed. The heating is dominated by the contribution from small scale structures of magnetic fields and thus it is important to resolve the cutoff scale of magnetic fields in Monte Carlo realizations. It should be noted that the spin temperature and ionization fraction fluctuations are positively correlated; namely, the region which has larger spin temperature has a larger ionization fraction. Consequently, the larger ionization fraction cancels out in part the contribution from the spin temperature to the 21cm brightness temperature, leading to smoother 21cm brightness temperature fluctuations.

Cross and auto power spectra of 21cm fluctuations are expressed as

$$\left\langle \prod_{i=1}^2 \delta T_{21}(\mathbf{k}_i, z_i) \right\rangle \equiv (2\pi)^3 P_{21}(k_1, z_1, z_2) \delta^{(3)}(\mathbf{k}_1 + \mathbf{k}_2) . \quad (12)$$

The power spectra are directly estimated from the simulations. In Fig. 2 we show the power spectra at  $z_1 = z_2 = 20$  for magnetic field strengths ranging from  $B_\lambda = 0$  nG to 1 nG, with the spectral index  $n_B = -2.9$  and 0.

The power spectrum of 21cm brightness temperature mainly has two parts. The one is coming from the temperature fluctuation term that is proportional to  $\delta(x_{\text{HI}}(T_s - T_\gamma)/T_s) \bar{n}_H$ , and the other is the density fluctuation term proportional to  $\bar{x}_{\text{HI}}(\bar{T}_s - \bar{T}_\gamma)/\bar{T}_s \delta n_H$ , where  $x_{\text{HI}} = n_{\text{HI}}/n_H = 1 - x_i$  is the neutral fraction and the bar means the average value. The former contribution to the power spectrum is estimated from the Monte Carlo simulations described earlier because of the complicated nonlinearity and denoted by  $P_{21}^s$ , while the latter can be estimated using a publicly available CMB code such as CAMB [59] and denoted by  $P_{21}^{\text{mat}}$ . Note that the latter contribution can be further divided into two contributions under the presence of magnetic fields. The Lorentz force acts on baryons and alters its density perturbations, while dark matters are indirectly affected by magnetic fields via the gravitational interaction with baryons. After cosmological recombination, an evolution equation for total matter fluctuations composed of baryon and dark matter fluctuations reads [41, 60]

$$\frac{d^2 \delta_m}{dt^2} = -2H \frac{d\delta_m}{dt} + 4\pi G \bar{\rho}_m \delta_m + \frac{\nabla \cdot [(\nabla \times \mathbf{B}) \times \mathbf{B}]}{4\pi \bar{\rho}_m a^2} , \quad (13)$$

where  $\bar{\rho}_m$  is the background total matter energy density and  $\delta_m$  is the density contrast of them. Solving Eq. (13) with the assumption that there is no correlation between primordial magnetic fields and primordial density fluctuations, the density matter power spectrum can be divided into two parts as

$$P_m(k) = P_m^{\text{CDM}}(k) + P_m^B(k) , \quad (14)$$

where the first term  $P_m^{\text{CDM}}(k)$  is originated from the primordial density fluctuations which are exactly the same as those in the standard  $\Lambda$ CDM model. The second term  $P_m^B$  represents the power spectrum of the density fluctuations produced by primordial magnetic fields which depends on the power spectrum of the magnetic fields, as shown in Ref. [61]. According to Eqs. (5) and (6), the power spectrum of 21cm fluctuations due to the density fluctuations can be given by

$$P_{21}^{\text{mat}}(k) = \delta \bar{T}_{21}^2 [P_m^{\text{CDM}}(k) + P_m^B(k)] \equiv P_{21}^{\text{CDM}}(k) + P_{21}^B(k) , \quad (15)$$

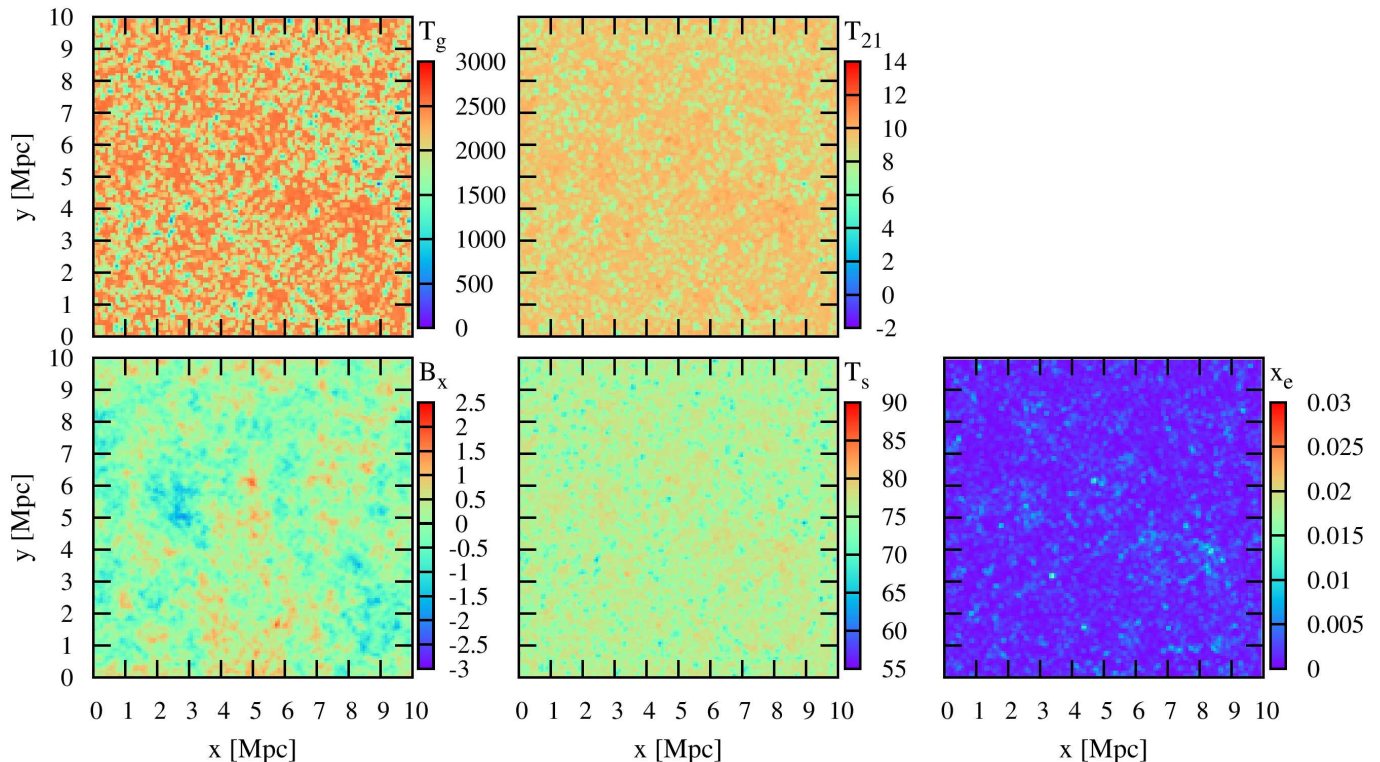


FIG. 1: Realization of (the  $x$  component of) primordial magnetic fields [nG] (bottom left) and corresponding fluctuations of the gas temperature [K] (top left), the spin temperature [K] (bottom center), the 21cm brightness temperature [mK] (top center), and the ionization fraction (bottom right) with parameters  $B_\lambda = 1$  [nG] and  $n_B = -2.9$ . The heating is dominated by contributions from small scale structures of magnetic fields. It can be seen that the spin temperature and the ionization fraction fluctuations are positively correlated.

where  $\delta\bar{T}_{21}$  is the mean differential brightness temperature obtained from Eqs. (5) and (6) with the background density  $\bar{n}_{\text{HI}}$  and the mean spin temperature  $\bar{T}_s$ .<sup>2</sup>

In Fig. 2, we separately plot these three contributions. We find that magnetic fields with nanogauss levels significantly enhance the power over the wide range of scales through the density fluctuation term  $P_{21}^{\text{mat}}$ , because they realize that  $(\bar{T}_s - \bar{T}_\gamma)/\bar{T}_{s|\text{PMF}} \sim 1 \gg (\bar{T}_s - \bar{T}_\gamma)/\bar{T}_{s|\text{no PMF}}$ , where the subscripts PMF and no PMF, respectively, represent the values with and without primordial magnetic fields, and give larger density fluctuations especially on small scales. If we consider the case with  $n_B = 0$ , even weaker magnetic fields with strength as small as  $B_\lambda = 10^{-3}$  nG can amplify the standard signal with no primordial magnetic fields (black dot-dashed line) by 3 orders of magnitude (see the right panel in the figure).

The contributions from the temperature fluctuations,  $P_{21}^s$ , are always subdominant for magnetic fields with a bluer spectrum, as shown in the right panel in Fig 2. However, the density fluctuations due to magnetic fields are suppressed below the magnetic Jeans scale. In the figure, to take into account this suppression, we introduce cutoffs to the contributions from  $P_m^B$ , namely,  $P_{21}^B$ , by hand at the magnetic Jeans scales. We find that  $P_{21}^s$  can give a comparable contribution with the primordial density fluctuation term,  $P_{21}^{\text{CDM}}$ , only on scales smaller than the cutoff scales for nearly scale-invariant magnetic fields ( $n_B = -2.9$ ; the left panel in the figure).

According to Eq. (1), as the magnetic field amplitude  $B_\lambda$  increases, the heating rate due to the ambipolar diffusion becomes large. However, when the gas temperature reaches  $T_g \sim 3000$  K, the temperature no longer rises and, instead, the ionization fraction grows. This ionization fraction growth suppresses the dissipation rate due to ambipolar diffusion as shown Eq. (1). As a result, the gas temperature remains  $T_g \sim 3000$  K and the ionization fraction gradually grows until the cosmological expansion term dominates in Eq. (2). During this regime, the fluctuations of the gas temperatures start to saturate, because the local gas temperature reaches 3000 K at many different places. Therefore,

<sup>2</sup> Although we ignore all cross-correlation terms, the cross correlation between the temperature and density fluctuations induced by magnetic fields can also contribute to the power spectrum  $P_{21}$ .

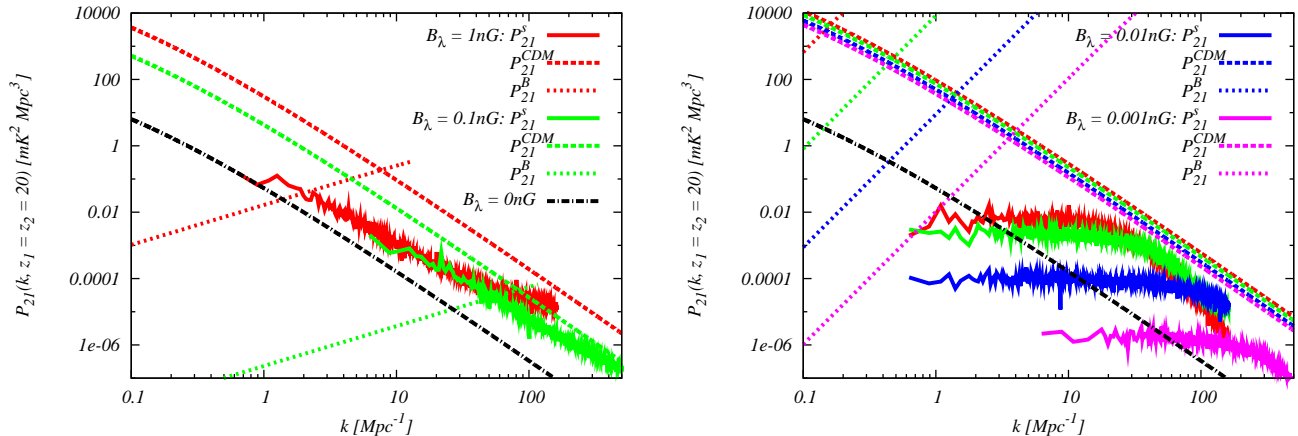


FIG. 2: Power spectra of the 21cm fluctuations for  $z_1 = z_2 = 20$  when  $n_B = -2.9$  (left) and 0 (right). Here,  $B_\lambda$  varies from 0 to 1 nG. For comparison, we separately plot the contributions from the temperature fluctuations ( $P_{21}^s$ : solid line), the standard matter fluctuations ( $P_{21}^{CDM}$ : dashed line), and the magnetized matter fluctuations ( $P_{21}^B$ : dotted line). Note that we here do not plot the 0.01 and 0.001 nG cases when  $n_B = -2.9$ , and the lines of  $P_{21}^s$  are broadened because it is one realization of the Monte Carlo simulations (also in Fig. 3).

when  $B_\lambda$  is large ( $B_\lambda > 0.1$  nG), the dependence of the  $P_{21}^s$  amplitude on  $B_\lambda$  becomes milder than in the cases with small  $B_\lambda$  as shown in Fig. 2.

#### IV. ANGULAR POWER SPECTRUM OF BRIGHTNESS TEMPERATURE FLUCTUATIONS

One of the main aims for 21cm observations is to measure the angular power spectrum (or three-dimensional power spectrum) of the 21cm fluctuations at each redshift. In this section, we evaluate the angular power spectra from the 21cm maps obtained in the previous section.

The 21cm fluctuations projected on a spherical shell at  $z = z_*$  with its width  $\Delta z_*$  are expressed as

$$\delta T_{21}(\hat{\mathbf{n}}, z_*, \Delta z_*) = \int_0^{\chi_\infty} d\chi W(\chi, \chi_*, \Delta\chi_*) \delta T_{21}(\mathbf{x}), \quad (16)$$

where  $\chi(z)$  denotes the conformal distance,  $\chi_* \equiv \chi(z_*)$ ,  $\chi_\infty \equiv \chi(\infty)$ ,  $\Delta\chi_* \equiv \chi(z_* + \frac{\Delta z_*}{2}) - \chi(z_* - \frac{\Delta z_*}{2})$ , and  $\hat{\mathbf{n}} \equiv \mathbf{x}/\chi_*$ . A normalized window function  $W(\chi, \chi_*, \Delta\chi_*)$  is associated with the bandwidth of an observation. Generally, the window function is a function of the frequency centered at the observed frequency. However, because there is one to one correspondence between the frequency and the conformal distance, we here adopt the following Gaussian function for simplicity,

$$W(\chi, \chi_*, \Delta\chi_*) = \frac{1}{\sqrt{2\pi(\Delta\chi_*/2)^2}} \exp\left[-\frac{(\chi - \chi_*)^2}{2(\Delta\chi_*/2)^2}\right]. \quad (17)$$

In this section, we shall analyze the angular power spectrum of  $\delta T_{21}(\hat{\mathbf{n}}, z_*, \Delta z_*)$  originating from primordial magnetic fields.

An expression in multipole space reads

$$\delta T_{21,\ell m}(z_*, \Delta z_*) = \int d^2\hat{\mathbf{n}} Y_{\ell m}^*(\hat{\mathbf{n}}) \delta T_{21}(\hat{\mathbf{n}}, z_*, \Delta z_*). \quad (18)$$

Under the assumption that 21cm signals are statistically isotropic, their angular power spectrum does not depend on  $m$ ,

$$\left\langle \prod_{i=1}^2 \delta T_{21,\ell_i m_i}(z_*, \Delta z_*) \right\rangle = (-1)^{m_1} \delta_{\ell_1 \ell_2} \delta_{m_1, -m_2} C_{\ell_1}(z_*, \Delta z_*), \quad (19)$$

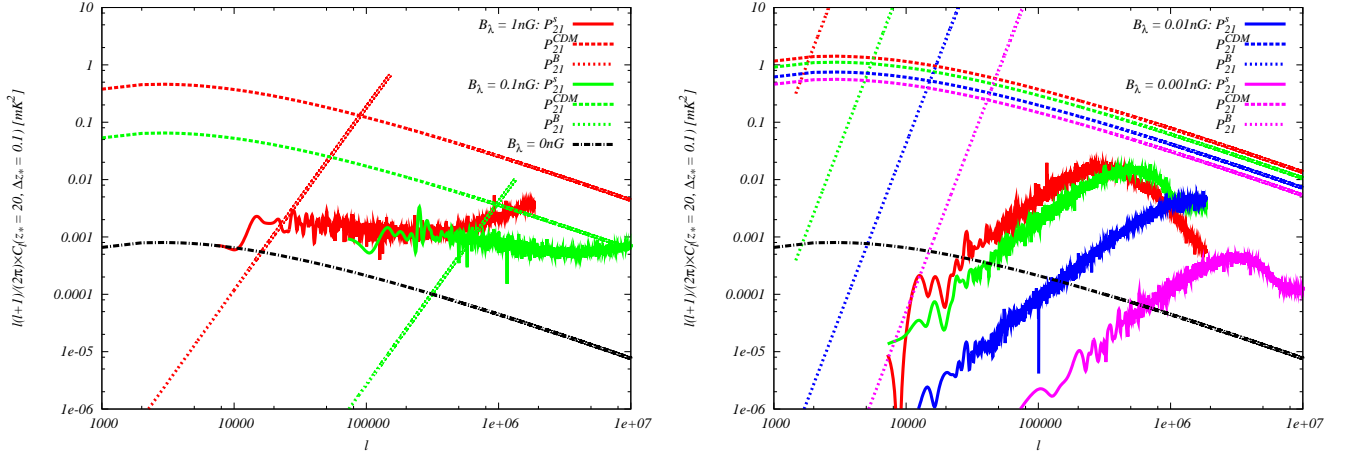


FIG. 3: Angular power spectra of the 21cm fluctuations for  $z_* = 20$  and  $\Delta z_* = 0.1$  when  $n_B = -2.9$  (left) and 0 (right). The settings are identical to Fig. 2.

and  $C_\ell$  is obtained by

$$C_\ell(z_*, \Delta z_*) = \frac{2}{\pi} \int_0^\infty k^2 dk \left[ \prod_{i=1}^2 \int_0^{\chi_\infty} d\chi_i W(\chi_i, \chi_*, \Delta\chi_*) j_\ell(k\chi_i) \right] P_{21}(k, z(\chi_1), z(\chi_2)). \quad (20)$$

For computations on small scales, a reduced formula under the flat-sky coordinate, namely,  $\hat{\mathbf{n}} \rightarrow (\boldsymbol{\theta}, 1)$ , is useful. The representations of  $\delta T_{21}$  and the angular power spectrum in  $\ell$  space are given by

$$\begin{aligned} \delta T_{21}(\boldsymbol{\ell}, z_*, \Delta z_*) &= \int d^2\boldsymbol{\theta} e^{-i\boldsymbol{\ell}\cdot\boldsymbol{\theta}} \delta T_{21}(\hat{\mathbf{n}}, z_*, \Delta z_*), \\ \left\langle \prod_{i=1}^2 \delta T_{21}(\boldsymbol{\ell}_i, z_*, \Delta z_*) \right\rangle &= (2\pi)^2 \delta^{(2)}(\boldsymbol{\ell}_1 + \boldsymbol{\ell}_2) C(\ell_1, z_*, \Delta z_*). \end{aligned} \quad (21)$$

Applying the so-called Limber approximation that Fourier waves along the  $z$  axis cancel each other out for  $\lambda \sim 1/k_z \ll \chi/\ell$  yields an expression for the angular power spectrum [62]:

$$C(\ell, z_*, \Delta z_*) = \int_0^{\chi_\infty} d\chi \frac{W^2(\chi, \chi_*, \Delta\chi_*)}{\chi^2} P_{21}\left(\frac{\ell}{\chi}, z(\chi), z(\chi)\right). \quad (22)$$

This is in good agreement with the exact formula (20) when the cancellations of Fourier waves happen frequently within the width of the window function, namely,  $\ell \gg \chi_*/\Delta\chi_*$ . The following numerical results focusing on such small scales are estimated by Eq. (22) because this enforces many fewer numerical operations than Eq. (20).

We plot the angular power spectra in Fig. 3. Similar to Fig. 2, we separately show the three contributions, the temperature fluctuations due to the ambipolar diffusion  $P_{21}^s$ , the primordial density fluctuations  $P_{21}^{\text{CDM}} = \delta\bar{T}_{21}^2 P_m^{\text{CDM}}$ , and the density fluctuations induced by magnetic fields  $P_{21}^B = \delta\bar{T}_{21}^2 P_m^B$ . Although  $P_m^{\text{CDM}}$  is independent from magnetic fields, the amplitude of  $P_{21}^{\text{CDM}}$  is sensitive to  $B_\lambda$  because magnetic fields increase the spin temperature through heating the background gas temperature due to the ambipolar diffusion.

For the power-law spectrum  $P_{21} \propto k^n$ , Eq. (22) tells us that the angular power spectrum  $\ell^2 C_\ell$  is proportional to  $\ell^{n+2}$ . Therefore, Fig. 3 shows that  $\ell^2 C_\ell$  due to  $P_{21}^s$  is proportional to  $\ell^{-0.1}$  and  $\ell^2$  for  $n_B = -2.9$  and 0, respectively, because the spectral index  $n$  of  $P_{21}^s$  is roughly  $n = -2.1$  for  $n_B = -2.9$  and  $n = 0$  for  $n_B = 0$ , as shown in Fig 2. We can also see that  $k$  space signatures are reflected in  $\ell$  space by following  $\ell \sim k\chi_*$  with  $\chi_* \sim 12$  Gpc.

As seen in Fig. 2,  $P_{21}^s$  is dominated by  $P_{21}^B$ . However, on smaller scales than the magnetic Jeans scale,  $P_{21}^B$  is expected to be strongly suppressed and the temperature fluctuations due to the ambipolar diffusion can significantly contribute to the 21cm signals with the primordial density fluctuation contributions, especially in the case with nearly scale-invariant magnetic fields ( $n_B = -2.9$ ; the left panel in the figure).

## V. CONCLUSION

In this paper, we have studied cosmological 21cm signals induced by primordial magnetic fields, focusing on the ambipolar diffusion of magnetic fields. The ambipolar diffusion heats the gas temperature and the heating rate depends on the magnetic field strength. Therefore, when primordial magnetic fields are tangled, the ambipolar diffusion not only increases the background gas temperature, but also generates the fluctuations of the gas temperature. These fluctuations alter the fluctuations of cosmological 21cm lines. We have evaluated these fluctuations due to the ambipolar diffusion, calculating the thermal evolution of the hydrogen gas with Monte Carlo simulations. We have shown that the 21cm fluctuations due to the ambipolar diffusion depend on the magnetic field properties such as the strength and the spectral index of magnetic fields. We have also found that the fluctuations start to saturate for the magnetic field strength  $B_\lambda > 0.1$  nG. This is because the gas temperature cannot increase beyond  $\sim 3000$  K due to the balance between the ionization fraction and the ambipolar diffusion rate. The gas temperatures in most regions reach this critical temperature for large  $B_\lambda$  and, as a result, the fluctuations cannot be amplified.

Primordial magnetic fields can give the other two effects on the 21cm fluctuations, as discussed in Refs. [43, 45]. One is the amplification of the 21cm fluctuations originating from the primordial density fluctuations because the dissipated magnetic field energy increases the background gas temperature. The other is the additional density fluctuations which are generated by primordial magnetic fields after the epoch of recombination. We have compared these two contributions with the contribution from the temperature fluctuations obtained by our simulations. Our result has shown that the contributions of the temperature fluctuations are subdominant on observation scales of future observations such as SKA. On these scales, the most important effect of primordial magnetic fields is the amplification due to the heating of the background gas temperature. This result is consistent with Refs. [43, 45]. The temperature fluctuation contribution can give the non-negligible contribution only on small scales ( $\ell > 10^5$ ) for nearly scale-invariant magnetic fields.

In this paper, we have focused on the effect of primordial magnetic fields on 21cm signals before the epoch of reionization. However, near future observations such as SKA are planned to observe the 21cm radiation during the epoch of reionization. In this paper, although we have taken into account the thermal ionization, we have not considered the photoionization by first stars and galaxies. The gas temperature heated by the dissipation of magnetic field energy modifies the Jeans mass [41, 44], and the additional density fluctuations due to primordial magnetic fields enhance the abundance of ionization photon sources [42, 44]. These effects are expected to modify the 21cm fluctuations from those in the standard  $\Lambda$ CDM model, and they can give a significant contribution to observable 21cm fluctuations. Therefore, to study the feasibility of the constraint on primordial magnetic fields by future observations, a detailed evaluation of these effects during the epoch of reionization is important. We leave this issue for a future work.

## Acknowledgments

M. S. is supported in part by a Grant-in-Aid for JSPS Research under Grant No. 25-573 and the ASI/INAF Agreement I/072/09/0 for the Planck LFI Activity of Phase E2. H. T. is supported by the DOE at Arizona State University. K. I. is also supported by Grant-in-Aid No. 24340048 from the Ministry of Education, Sports, Science and Technology of Japan

- 
- [1] L. M. Widrow, *Reviews of Modern Physics* **74**, 775 (2002).
  - [2] L. M. Widrow, D. Ryu, D. R. G. Schleicher, K. Subramanian, C. G. Tsagas, and R. A. Treumann, *Space Sci. Rev.* **166**, 37 (2012), 1109.4052.
  - [3] R. Durrer and A. Neronov, *A&A Rev.* **21**, 62 (2013), 1303.7121.
  - [4] A.-C. Davis, M. Lilley, and O. Törnkvist, *Phys. Rev. D* **60**, 021301 (1999).
  - [5] B. Ratra, *Astrophys. J.* **391**, L1 (1992).
  - [6] M. S. Turner and L. M. Widrow, *Phys. Rev. D* **37**, 2743 (1988).
  - [7] A.-C. Davis, K. Dimopoulos, T. Prokopec, and O. Törnkvist, *Physics Letters B* **501**, 165 (2001), arXiv:astro-ph/0007214.
  - [8] K. Bamba and J. Yokoyama, *Phys. Rev. D* **69**, 043507 (2004), arXiv:astro-ph/0310824.
  - [9] J. Martin and J. Yokoyama, *J. Cosmology Astropart. Phys.* **1**, 025 (2008), 0711.4307.
  - [10] T. Suyama and J. Yokoyama, *Phys. Rev. D* **86**, 023512 (2012), 1204.3976.
  - [11] T. Fujita and S. Mukohyama, *J. Cosmology Astropart. Phys.* **10**, 034 (2012), 1205.5031.
  - [12] C. J. Hogan, *Physical Review Letters* **51**, 1488 (1983).
  - [13] T. Vachaspati, *Physics Letters B* **265**, 258 (1991).



- [14] M. Hindmarsh and A. Everett, *Phys. Rev. D* **58**, 103505 (1998), arXiv:astro-ph/9708004.
- [15] J. Ahonen and K. Enqvist, *Phys. Rev. D* **57**, 664 (1998), arXiv:hep-ph/9704334.
- [16] E. M. Henley, M. B. Johnson, and L. S. Kisslinger, *Phys. Rev. D* **81**, 085035 (2010), 1001.2783.
- [17] T. Kahniashvili, A. G. Tevzadze, A. Brandenburg, and A. Neronov, *Phys. Rev. D* **87**, 083007 (2013), 1212.0596.
- [18] A. J. Long, E. Sabancilar, and T. Vachaspati, *J. Cosmology Astropart. Phys.* **2**, 036 (2014), 1309.2315.
- [19] K. Takahashi, K. Ichiki, H. Ohno, and H. Hanayama, *Physical Review Letters* **95**, 121301 (2005), arXiv:astro-ph/0502283.
- [20] K. Ichiki, K. Takahashi, H. Ohno, H. Hanayama, and N. Sugiyama, *Science* **311**, 827 (2006), arXiv:astro-ph/0603631.
- [21] S. Maeda, S. Kitagawa, T. Kobayashi, and T. Shiromizu, *Classical and Quantum Gravity* **26**, 135014 (2009), 0805.0169.
- [22] K. Ichiki, K. Takahashi, N. Sugiyama, H. Hanayama, and H. Ohno, *ArXiv Astrophysics e-prints* (2007), arXiv:astro-ph/0701329.
- [23] E. Fenu, C. Pitrou, and R. Maartens, *MNRAS* **414**, 2354 (2011), 1012.2958.
- [24] S. Matarrese, S. Mollerach, A. Notari, and A. Riotto, *Phys. Rev. D* **71**, 043502 (2005).
- [25] E. R. Harrison, *MNRAS* **147**, 279 (1970).
- [26] C. J. Hogan (2000), astro-ph/0005380.
- [27] R. Gopal and S. K. Sethi, *MNRAS* **363**, 521 (2005).
- [28] Z. Berezhiani and A. D. Dolgov, *Astroparticle Physics* **21**, 59 (2004).
- [29] S. Saga, M. Shiraishi, K. Ichiki, and N. Sugiyama, *Phys. Rev. D* **87**, 104025 (2013), 1302.4189.
- [30] K. Ichiki, K. Takahashi, and N. Sugiyama, *Phys. Rev. D* **85**, 043009 (2012), 1112.4705.
- [31] M. L. Bernet, F. Miniati, S. J. Lilly, P. P. Kronberg, and M. Dessauges-Zavadsky, *Nature* **454**, 302 (2008), 0807.3347.
- [32] R. Joshi and H. Chand, *ArXiv e-prints* (2013), 1307.2678.
- [33] A. Neronov, D. Semikoz, and M. Banafsheh, *ArXiv e-prints* (2013), 1305.1450.
- [34] A. Neronov and I. Vovk, *Science* **328**, 73 (2010), 1006.3504.
- [35] S. Ando and A. Kusenko, *ApJ* **722**, L39 (2010), 1005.1924.
- [36] K. Takahashi, M. Mori, K. Ichiki, S. Inoue, and H. Takami, *ApJ* **771**, L42 (2013), 1303.3069.
- [37] K. Takahashi, M. Mori, K. Ichiki, and S. Inoue, *ApJ* **744**, L7 (2012), 1103.3835.
- [38] F. Tavecchio, G. Ghisellini, G. Bonnoli, and L. Foschini, *MNRAS* **414**, 3566 (2011), 1009.1048.
- [39] D. G. Yamazaki, T. Kajino, G. J. Mathews, and K. Ichiki, *Phys. Rep.* **517**, 141 (2012), 1204.3669.
- [40] Planck Collaboration, P. A. R. Ade, N. Aghanim, C. Armitage-Caplan, M. Arnaud, M. Ashdown, F. Atrio-Barandela, J. Aumont, C. Baccigalupi, A. J. Banday, et al., *ArXiv e-prints* (2013), 1303.5076.
- [41] S. K. Sethi and K. Subramanian, *MNRAS* **356**, 778 (2005), arXiv:astro-ph/0405413.
- [42] H. Tashiro and N. Sugiyama, *MNRAS* **368**, 965 (2006), arXiv:astro-ph/0512626.
- [43] H. Tashiro and N. Sugiyama, *MNRAS* **372**, 1060 (2006), arXiv:astro-ph/0607169.
- [44] D. R. G. Schleicher, R. Banerjee, and R. S. Klessen, *Phys. Rev. D* **78**, 083005 (2008), 0807.3802.
- [45] D. R. G. Schleicher, R. Banerjee, and R. S. Klessen, *ApJ* **692**, 236 (2009), 0808.1461.
- [46] K. E. Kunze and E. Komatsu, *ArXiv e-prints* (2013), 1309.7994.
- [47] F. H. Shu, *Physics of Astrophysics, Vol. II* (University Science Books, 1992).
- [48] T. G. Cowling, *MNRAS* **116**, 114 (1956).
- [49] B. T. Draine, W. G. Roberge, and A. Dalgarno, *ApJ* **264**, 485 (1983).
- [50] S. Seager, D. D. Sasselov, and D. Scott, *ApJ* **523**, L1 (1999), arXiv:astro-ph/9909275.
- [51] S. Seager, D. D. Sasselov, and D. Scott, *ApJS* **128**, 407 (2000), arXiv:astro-ph/9912182.
- [52] P. Madau, A. Meiksin, and M. J. Rees, *ApJ* **475**, 429 (1997), astro-ph/9608010.
- [53] S. A. Wouthuysen, *AJ* **57**, 31 (1952).
- [54] G. B. Field, *Proceedings of the IRE* **46**, 240 (1958).
- [55] J. R. Shaw and A. Lewis, *Phys. Rev. D* **81**, 043517 (2010), 0911.2714.
- [56] T. Kahniashvili, A. G. Tevzadze, S. K. Sethi, K. Pandey, and B. Ratra, *Phys.Rev.* **D82**, 083005 (2010), 1009.2094.
- [57] K. Jedamzik, V. Katalinic, and A. V. Olinto, *Phys.Rev.* **D57**, 3264 (1998), astro-ph/9606080.
- [58] K. Subramanian and J. D. Barrow, *Phys.Rev.* **D58**, 083502 (1998), astro-ph/9712083.
- [59] A. Lewis and A. Challinor, *Phys.Rev.* **D76**, 083005 (2007), astro-ph/0702600.
- [60] E.-J. Kim, A. V. Olinto, and R. Rosner, *ApJ* **468**, 28 (1996), arXiv:astro-ph/9412070.
- [61] J. R. Shaw and A. Lewis, *Phys. Rev. D* **86**, 043510 (2012), 1006.4242.
- [62] S. Dodelson, *Modern cosmology* (2003).